Peer-reviewed version available at *Membranes* **2018**, *8*, 124; doi:10.3390/membranes8040124

Towards biohydrogen separation using poly(ionic liquid)/ionic liquid composite membranes

Andreia S.L. Gouveia,[a,b] Lucas Ventaja,[a] Liliana C. Tomé,[a,b] and Isabel M. Marrucho[a,b]**

[a] Centro de Química Estrutural, Instituto Superior Técnico, Universidade de Lisboa, Avenida Rovisco Pais, 1049-001 Lisboa, Portugal

[b] Instituto de Tecnologia Química e Biológica António Xavier, Universidade Nova de Lisboa, Av. da República, 2780-157 Oeiras, Portugal

***Corresponding Authors**

isabel.marrucho@tecnico.ulisboa.pt. Fax: +351 21 8499242. Tel: +351 21 8413385
liliana.tome@itqb.unl.pt. Fax: +351 21 4411277. Tel: +351 21 4469714

Peer-reviewed version available at Membranes 2018, 8, 124; doi:10.3390/membranes8040124

ABSTRACT

Considering the high potential of hydrogen (H_2) as a clean energy carrier, the implementation of high performance and cost-effective biohydrogen (bioH_2) purification techniques is of vital importance, particularly in fuel cell applications. In this context, membrane technology is a potentially energy-saving solution to obtain high-quality biohydrogen.

The most promising poly(ionic liquid) (PIL) - ionic liquid (IL) composite membranes previously studied by our group for CO_2/N_2 separation, containing pyrrolidinium-based PILs with fluorinated or cyano-functionalized anions, were chosen as starting point to explore the potential of PIL–IL membranes for CO_2/H_2 separation. The CO_2 and H_2 permeation properties at the typical conditions of biohydrogen production (T =308 K and 100 kPa of feed pressure) were measured and discussed. PIL–IL composites prepared with $[C(CN)_3]^-$ anion showed higher CO_2/H_2 selectivities and H_2 diffusivities compared to those containing $[NTf_2]^-$ anion. All the membranes revealed CO_2/H_2 separation performances above the upper bound for this specific separation, highlighting the composite incorporating 60 wt% of $[C_2mim][C(CN)_3]$ IL.

KEYWORDS

Biohydrogen purification, CO_2/H_2 separation, PIL–IL composite membranes, Gas permeation properties.

Peer-reviewed version available at Membranes 2018, 8, 124; doi:10.3390/membranes8040124

1. INTRODUCTION

Due to its outstanding intrinsic features, hydrogen (H_2) has been considered the energy carrier of the future. Besides being the simplest element in the universe, H_2 molecule has the highest energy content per unit weight of any known fuel. However, H_2 is not a primary fuel source, which means that it is not available in nature and thus needs to be produced [1]. Hydrogen has been mainly produced at an industrial scale from fossil fuels, through natural gas reforming or coal gasification, and from water, using electrolysis, in which water (H_2O) can be split into hydrogen and oxygen (O_2) [2]. Although water splitting is an ecologically clean process compared to the previously mentioned H_2 production processes, it is a highly energy-demanding technology [3].

Hydrogen production using biological processes has been attracting growing attention, since it is more environmentally friendly and less energy intensive as their operation conditions are close to room temperature (303 – 313 K) and ambient pressure (100 kPa) [2]. BioH_2 production can be divided into two main different categories, light dependent (direct or indirect biophotolysis and photo fermentation) and independent (dark fermentation) methodologies [4-6]. Dark fermentation process has several advantages compared to the other biological processes, namely its potential for cost-effective hydrogen production, the high rate of cell growth and non-requirement of light energy [6]. Albeit the recognized potential of biohydrogen for a sustainable development, there are still pending issues regarding its production and purification [7], as the elimination of CO_2, N_2 and other impurities (H_2O and H_2S), so that an enriched H_2 stream can be obtained for efficient energy generation, mostly through fuel cells [8]. Among the several methodologies to separate hydrogen, such as pressure swing adsorption (PSA), cryogenic distillation and membrane separation, the first two are mainly designed for large-scale hydrogen

production and cannot be used without modification for upgrade of relatively small amounts of biohydrogen [9]. Thus, membrane technology has been reported as an attractive alternative for biohydrogen separation and purification [10], since they can easily be introduced in hydrogen producing bioreactors, leading to an integrated process of bioH_2 production and purification [11,12], not omitting their important engineering and economic advantages. Particularly, polymeric membranes, such as polysulfone (PSF) or polyimide (PI) [13], have been considered a suitable choice for biohydrogen separation as they can not only be used at the bioreactors operation conditions but also due to their low cost, high energy efficiency and smaller ecological footprint compared to conventional separation processes [14-16].

Few articles have been published using membranes for bioH_2 separation. Among them, the blending of different polymers and ionic liquids (ILs) to prepare polymeric composite membranes is one of the most promising approaches, which takes into account the inherent CO_2 philicity of ILs [17]. For instance, S. Kanehashi et al. [18] prepared different composite membranes based on a fluorine-containing polyimide with different amounts of [C_4mim][NTf_2] IL up to 81 wt%, and studied their gas separation performance at 308 K and 100 kPa of feed pressure. These authors showed that the highest CO_2/H_2 permselectivity (6.6) was obtained for the membrane comprising the maximum amount of IL (81 wt%) [18]. Moreover, Friess et al. [19] studied the gas permeation properties at 298 K and 100 kPa of feed pressure through polymeric membranes composed of poly(vinylidene fluoride-co-hexafluoropropylene) and 20 to 80 wt% of [C_2mim][NTf_2] IL. Again, the largest CO_2 permeability (533 Barrer) and CO_2/H_2 permselectivity (12.1) were obtained when the highest amount of IL (80 wt%) was used [19].

With the aim of designing efficient CO_2/H_2 separation membranes, this work explores the use

Peer-reviewed version available at Membranes 2018, 8, 124; doi:10.3390/membranes8040124

of poly(ionic liquid)s (PILs), which are well recognized by their high CO_2-affinity and designer nature [20]. Different approaches have been proposed to produce PIL-based CO_2 separation membranes, such as neat PIL membranes [21-24], PIL copolymer membranes [20,25], the incorporation of ILs alone or together with nanoporous materials as fillers, including zeolites or metal organic frameworks (MOFs), to form PIL/IL/filler mixed matrix membranes (MMMs) [26-28]. Among all these, the blending of PILs and ILs to produce homogeneous PIL–IL composite membranes is the most promising not only due to the good CO_2 separation performances, but also the high mechanical stability of the membranes [29]. Notwithstanding the potential of PILs for CO_2 separation [29-33], only a reduced number of works concerning CO_2/H_2 separation have been reported in literature. For instance, Carlisle *et al.* [34] explored the CO_2/H_2 separation through imidazolium PIL–IL gel membranes produced by UV polymerization. The time-lag experiments performed at room temperature and 200 kPa of feed pressure show ideal CO_2/H_2 selectivities ranging from 6.6. to 12 for membranes prepared with 5 to 100 mol% of a cross-linking monomer and the different amounts of free IL and IL monomer. In fact, their best result (CO_2 permeability of 540 Barrer and CO_2/H_2 selectivity of 12) was achieved for the composite containing 100 mol% of cross-linking monomer and 75 wt% of IL [34]. Moreover, Kharul *et al.* [35] studied the CO_2 and H_2 separation properties of polybenzimidazole-based PILs. The different synthesized polybenzimidazole-based PILs exhibited very similar CO_2 and H_2 permeabilities (< 30 Barrer), and consequently CO_2/H_2 selectivities approximately equal to 1 [35].

Amongst the PIL–IL composite membranes developed so far for CO_2/N_2 separation, the most widely explored are those composed of imidazolium-based PILs with fluorinated or cyano-functionalized anions [36-38]. However, our group reported that PIL–IL membranes, made of

pyrrolidinium-based PILs combining the same anions, which are particularly simple to prepare, through a metathesis reaction of a commercially available polymer, which display CO_2/N_2 separation performances near or even above the Robeson upper bound [39-42]. In fact, the CO_2-phylic behavior of $[NTf_2]^-$ anion and the CO_2 separation efficiency of $[C(CN)_3]^-$ anion [43] motivated us to explore the most promising pyrrolidinium-based PIL–IL composites containing these two anions for CO_2/N_2 separation, now for CO_2/H_2 separation.

In this work, solvent casting method was used to prepare composite membranes composed of two pyrrolidinium-based PILs, poly($[Pyr_{11}][NTf_2]$) and poly($[Pyr_{11}][C(CN)_3]$). The poly($[Pyr_{11}][NTf_2]$) was blended with 40 and 60 wt% of the structurally similar $[C_4mpyr][NTf_2]$ IL and also with 40 wt% of an imidazolium-based IL ($[C_2mim][NTf_2]$), while poly($[Pyr_{11}][C(CN)_3]$) was mixed with 40 and 60 wt% of $[C_2mim][C(CN)_3]$ IL. The chemical structures of the PILs and ILs used are shown in Figure 1. The CO_2 and H_2 permeation properties (permeability, diffusivity and solubility) were determined at two different temperatures (T = 293 K and T = 308 K) under a transmembrane pressure differential of 100 kPa. The temperature of 293 K was first used so that the results obtained herein can be compared to those previously reported by our group and thus confirm the reproducibility of the used method, while T = 308 K was chosen to reproduce the hydrogen bioproduction conditions [13].

Preprints (www.preprints.org) | NOT PEER-REVIEWED | Posted: 22 October 2018 doi:10.20944/preprints201810.0467.v1

Peer-reviewed version available at Membranes 2018, 8, 124; doi:10.3390/membranes8040124

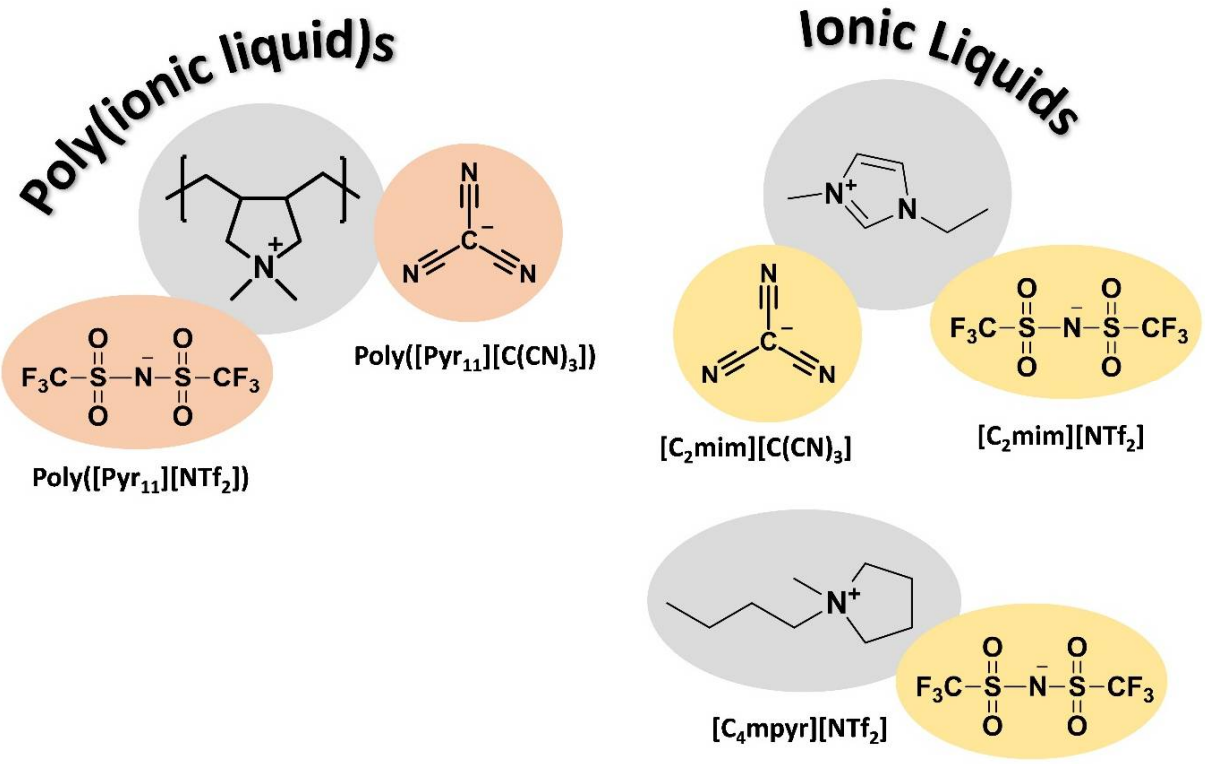

Figure 1 Chemical structures of the PILs and ILs used in this work to prepare the PIL–IL membranes.

2. EXPERIMENTAL SECTION

2.1. Materials. Poly(diallyldimethylammonium) chloride solution (average M_w 400,000 – 500,000, 20 wt% in water), acetone (99.8%) and acetonitrile (99.8%) were purchased from Sigma-Aldrich. Lithium bis(trifluoromethylsulfonyl)imide ($LiNTf_2$, 99 wt% pure) and sodium tricyanomethanide ($NaC(CN)_3$, 98 wt% pure) were supplied by IoLiTec GmbH. The PILs used were previously synthesized by anion metathesis reactions, as described elsewhere [40,44], and all the starting materials of their synthesis, as well as the organic solvents, were used as received. The water was double distilled. The ILs, 1-ethyl-3-methylimidazolium tricyanomethanide ($[C_2mim][C(CN)_3]$, > 98 wt% pure), 1-ethyl-3-methylimidazolium

Peer-reviewed version available at Membranes 2018, 8, 124; doi:10.3390/membranes8040124

bis(trifluoromethylsulfonyl)imide ([C_2mim][NTf_2], > 99 wt% pure) and 1-butyl-1-methylpyrrolidinium bis(trifluoromethylsulfonyl)imide ([C_4mpyr][NTf_2], > 99 wt% pure) were provided by IoLiTec GmbH. Carbon dioxide (CO_2) and hydrogen (H_2) were supplied by Air Liquide with a minimum purity of 99.99%. Gases were used with no further purification.

2.2. Preparation of PIL–IL Membranes. Several free-standing membranes based on the synthesized PILs and specific quantities of different ILs containing the same anions were prepared by solvent casting. First, 6 (w/v)% and 12 (w/v)% solutions of poly([Pyr_{11}][$C(CN)_3$]) and poly([Pyr_{11}][NTf_2]), respectively, in appropriate solvents were prepared and the respective IL amounts were added (Table 1). The solutions were magnetically stirred, until complete dissolution of PIL and IL components, before being poured into Petri dishes and left for slow evaporation of the solvent for 2/3 days, depending on the solvent used (Table 1), at room temperature. A digital micrometer (Mitutoyo, model MDE-25PJ, Japan) was used to measure the thicknesses of the prepared membranes (70–210 μm). Average thickness was calculated from six measurements taken at different locations of each PIL–IL membrane.

Table 1 Composition descriptions and experimental conditions of the casting procedure used to prepare the PIL–IL composite membranes.

PIL-IL membrane	Polymer (PIL)	wt% of IL	Solvent	*T* (K)	Evaporation time (days)
PIL $C(CN)_3$ – 40 [C_2mim][$C(CN)_3$]	Poly([Pyr_{11}][$C(CN)_3$])	40	Acetonitrile	298	3
PIL $C(CN)_3$ – 60 [C_2mim][$C(CN)_3$]		60			
PIL NTf_2 – 40 [C_4mpyr][NTf_2]	Poly([Pyr_{11}][NTf_2])	40	Acetone	298	2
PIL NTf_2 – 60 [C_4mpyr][NTf_2]		60			
PIL NTf_2 – 40 [C_2mim][NTf_2]	Poly([Pyr_{11}][NTf_2])	40	Acetone	298	2

Peer-reviewed version available at Membranes 2018, 8, 124; doi:10.3390/membranes8040124

2.4. Gas Permeation Experiments. Ideal CO_2 and H_2 permeabilities and diffusivities through the PIL–IL membranes were measured using a time-lag equipment, described in detail elsewhere [39]. Initially, each membrane was degassed under vacuum inside the permeation cell during at least 12 h before testing. The gas permeation measurements were performed at 293 K and 308 K with an upstream pressure of 100 kPa (feed) and vacuum (< 0.1 kPa) as the initial downstream pressure (permeate). Three separate CO_2 and H_2 experiments on a single membrane sample were measured. Between each run, the permeation cell and lines were evacuated until the pressure was below 0.1 kPa. At the end of the gas experiments, no residual IL was found inside the permeation cell.

The gas transport through PIL–IL composite membranes was assumed to occur according to solution-diffusion mass transfer mechanism [45]. Thus, the permeability (P) is related to diffusivity (D) and solubility (S) as follows:

$$P = D \times S \tag{1}$$

The permeate flux of each studied gas (J_i) was experimentally determined using Eq. (2) and assuming an ideal gas behavior and a homogeneous membrane [46].

$$J_i = \frac{V^p \Delta p_d}{AtRT} \tag{2}$$

where V^p is the permeate volume, Δp_d is the variation of downstream pressure, A is the effective membrane surface area, t is the experimental time, R is the Gas Constant and T is the temperature. Ideal gas permeability (P_i) was then calculated from the pressure driving force (Δp_i) and membrane thickness (ℓ) as shown in Eq. (3).

$$P_i = \frac{J_i}{\Delta_{pi}/\ell} \tag{3}$$

Peer-reviewed version available at Membranes 2018, 8, 124; doi:10.3390/membranes8040124

Eq. (4) was used to determine gas diffusivity (D_i). The time-lag parameter (θ) was deduced by extrapolating the slope of the linear portion of the p_d vs. t curve back to the time axis, where the intercept is equal to θ [47].

$$D_i = \frac{\ell^2}{6\theta} \tag{4}$$

Gas solubility (S_i) was also calculated using the relationship given by Eq. (1), after defining both P_i and D_i.

The ideal permeability selectivity (or permselectivity), $\alpha_{i/j}$, which can also be expressed as the product of the diffusivity selectivity and the solubility selectivity was obtained by dividing the permeability of the more permeable specie i to the permeability of the less permeable specie j, as represented in Eq. (5).

$$\alpha_{i/j} = \frac{P_i}{P_j} = \left(\frac{D_i}{D_j}\right) \times \left(\frac{S_i}{S_j}\right) \tag{5}$$

3. RESULTS AND DISCUSSION

3.1. CO_2 and H_2 permeation properties

3.1.1. Gas Permeability (*P*)

The measured CO_2 and H_2 permeabilities, at 293 K and 308 K, through the studied PIL-IL composite membranes are plotted in Figure 2. The CO_2 permeability is always higher than that of H_2 and both permeabilities increase with increasing temperature, although the increment is not the same between the studied composites, varying from 15 to 50% for CO_2 permeability values and from 39 to 77% for H_2 permeabilities. It is worth noting that the CO_2 permeabilities at 293 K for all the membranes here discussed are in good agreement with those already reported by our

Peer-reviewed version available at Membranes 2018, 8, 124; doi:10.3390/membranes8040124

group [39,40,42], which emphasizes the high reproducibility of the used method. As expected, the incorporation of high amount of IL leads to enhanced CO_2 and H_2 permeabilities. Additionally, at 308 K, the temperature of bioH_2 purification, the composite membrane PIL NTf_2 – 40 [C_2mim][NTf_2] presents similar CO_2 and H_2 permeability values to those of PIL NTf_2 – 60 [C_4mpyr][NTf_2] membrane. This means that despite the higher structural compatibility of [C_4mpyr][NTf_2] with the pyrrolidinium-based PIL, the imidazolium-based cation of the IL is determinant to promote increased gas permeabilities. However, and as already reported by our group [42], the use of [C_2mim][NTf_2] instead of [C_4mpyr][NTf_2] only allowed the incorporation of free IL up to 40 wt% so that an homogeneous membrane can be attained. Considering the PIL–IL membranes that have the $[C(CN)_3]^-$ anion in both PIL and IL, it can be observed that the PIL $C(CN)_3$ – 60 [C_2mim][$C(CN)_3$] composite shows the highest CO_2 permeability (505 Barrer) at 308 K, but not the highest H_2 permeability (40.3 Barrer), which was obtained for PIL NTf_2 – 60 [C_4mpyr][NTf_2] composite membrane (46.0 Barrer). Moreover, CO_2 permeability increased about 42%, while H_2 permeability increased approximately 57%, when the IL content in the PIL $C(CN)_3$ – [C_2mim][$C(CN)_3$] composite varies from 40 to 60 wt%. On the other hand, a significant difference in CO_2 permeability (76%) was obtained for the PIL–IL membranes comprising [C_4mpyr][NTf_2] IL when IL amount increased from 40 to 60 wt%, while the increase in H_2 permeability was only around 34%.

Preprints (www.preprints.org) | NOT PEER-REVIEWED | Posted: 22 October 2018 doi:10.20944/preprints201810.0467.v1

Peer-reviewed version available at Membranes 2018, 8, 124; doi:10.3390/membranes8040124

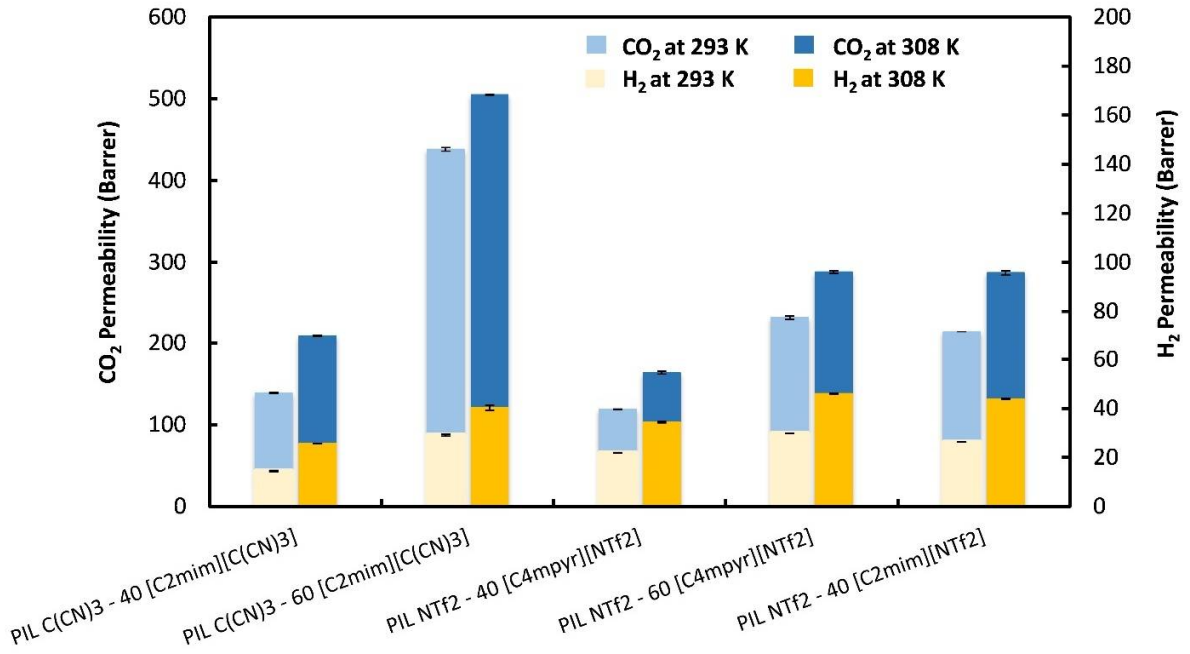

Figure 2 Experimental CO_2 and H_2 permeabilities (*P*) through the prepared PIL–IL membranes. Error bars represent standard deviations based on three experimental replicas.

3.1.2. Gas Diffusivity (*D*)

The experimental gas diffusivity results at 293 K and 308 K through the prepared membranes are listed in Table 2. A high difference (one or, in some cases, two orders of magnitude) between CO_2 diffusivity values and H_2 diffusivities, which corresponds to CO_2/H_2 diffusivity selectivities around 0.1, can be observed. This difference in gas diffusivities is mainly due to the smaller size of H_2 (2.89 Å) compared to CO_2 kinetic diameter (3.30 Å) [48]. Moreover, both CO_2 and H_2 diffusivity increases with increasing temperature and with increasing IL content in the PIL-IL composite (Table 2). The same behavior was also found for CO_2 and H_2 permeabilities (Figure 2). From Table 2, it can also be observed that CO_2 and H_2 diffusivities through the prepared membranes can be ordered as follows: PIL NTf_2 – 40 [C_4mpyr][NTf_2] < PIL NTf_2 – 60

[C_4mpyr][NTf_2] < PIL NTf_2 – 40 [C_2mim][NTf_2] < PIL $C(CN)_3$ – 40 [C_2mim][$C(CN)_3$] < PIL $C(CN)_3$ – 60 [C_2mim][$C(CN)_3$]. The same trend was also observed for N_2 diffusivities in the same PIL-IL membranes already reported by our group [39,40,42]. Thus, and as expected, it can be concluded that gas diffusivities follow the order of the kinetic diameters $CO_2 < N_2 < H_2$.

Another interesting point is the comparison between gas permeabilities and diffusivities behavior. Regardless of the anion, although the composite that comprises 60 wt% of IL has the highest H_2 diffusivities (> 1200 $m^2 s^{-1}$ at 308 K), it does not present the highest H_2 permeabilities (Figure 2). An equivalent behavior was also obtained for PIL NTf_2 – 40 [C_4mpyr][NTf_2] composite membrane, that displays the lowest H_2 diffusivities (546 $m^2 s^{-1}$ at 308 K) but not the lowest H_2 permeabilities (Figure 2). In the case of CO_2, it can be seen from Table 2 and Figure 2, that CO_2 permeability follows the same trend of CO_2 diffusivity, with the exception of PIL NTf_2 – 60 [C_4mpyr][NTf_2] and PIL $C(CN)_3$ – 40 [C_2mim][$C(CN)_3$] membranes. This behavior led us to conclude that the very high difference (three or, in some cases, four orders of magnitude) among H_2 diffusivities is somehow compensated by a reverse behavior in H_2 solubilities (as it will be discussed in the next section), which has a significant impact in H_2 permeability results.

Preprints (www.preprints.org) | NOT PEER-REVIEWED | Posted: 22 October 2018 doi:10.20944/preprints201810.0467.v1

Peer-reviewed version available at Membranes 2018, 8, 124; doi:10.3390/membranes8040124

Table 2 Experimental gas diffusivities (*D*) through the studied PIL–IL membranes at $T = 293$ K and $T = 308$ K.

PIL-IL membrane	Gas Diffusivity (x 10^{12}) ($m^2 s^{-1}$) ($T = 293$ K)		Gas Diffusivity (x 10^{12}) ($m^2 s^{-1}$) ($T = 308$ K)	
	D $CO_2 \pm \sigma$	D $H_2 \pm \sigma$	D $CO_2 \pm \sigma$	D $H_2 \pm \sigma$
PIL $C(CN)_3$ – 40 $[C_2mim][C(CN)_3]$	64 ± 1.0	970 ± 36.2	112 ± 2.5	1146 ± 34.0
PIL $C(CN)_3$ – 60 $[C_2mim][C(CN)_3]$	127 ± 1.1	1130 ± 5.70	181 ± 0.6	1211 ± 3.2
PIL NTf_2 – 40 $[C_4mpyr][NTf_2]$	34 ± 0.1	484 ± 18.5	62 ± 1.8	546 ± 20.6
PIL NTf_2 – 60 $[C_4mpyr][NTf_2]$	44 ± 0.7	610 ± 6.30	76 ± 0.5	673 ± 16.9
PIL NTf_2 – 40 $[C_2mim][NTf_2]$	61 ± 0.4	722 ± 1.80	106 ± 1.5	792 ± 3.70

3.1.3. Gas Solubility (*S*)

Gas solubility (*S*) values were calculated using Eq. 1, at both temperatures of 293 K and 308 K and are displayed in Figure 3. The CO_2 solubility decreases with increasing temperature, while H_2 solubility increases with increasing temperature, for all the studied PIL–IL membranes. Analogous reverse H_2 solubility behavior with temperature was also found and discussed by Raeissi et al. [49] in imidazolium-based ILs, such as $[C_4mim][NTf_2]$, which means that hydrogen dissolves better at higher than at lower temperatures. This trend seems to be the general rule for H_2 solubility in ILs, [49-53] and has been attributed to the extreme lightness and small intermolecular forces of hydrogen molecules. [49] Moreover, the large differences between CO_2 and H_2 solubilities can be explained by the high CO_2 critical temperature (CO_2, 31ºC; H_2, -240ºC), corresponding to a superior condensability of CO_2 ($T_{\varepsilon/k} = 195.2$ K) compared to that of H_2 ($T_{\varepsilon/k} = 59.7$ K) [48,54]. The fact that H_2 can almost be considered an ideal gas, due to its small kinetic diameter and non-interacting nature, while CO_2 displays a higher kinetic diameter and a

Preprints (www.preprints.org) | NOT PEER-REVIEWED | Posted: 22 October 2018 doi:10.20944/preprints201810.0467.v1

Peer-reviewed version available at Membranes 2018, 8, 124; doi:10.3390/membranes8040124

quadrupole moment also plays a role in the difference in solubilities of the two gases. For the PIL-IL composites studied in this work at 308 K, the CO_2 solubility ranges from 14 to 28.5 (x 10^{-6}) $m^3_{(STP)}$ m^{-3} Pa^{-1}, whereas H_2 solubility values are two orders of magnitude lower, varying from 0.17 to 0.51 (x 10^{-6}) $m^3_{(STP)}$ m^{-3} Pa^{-1}. Among all the tested membranes, the PIL NTf_2 – 60 [C_4mpyr][NTf_2] composite presents the highest CO_2 and H_2 solubilities, at both 293 and 308 K. Regarding the influence of anion's structure, and considering the same amount of free IL in the composite, it can be concluded that the presence of the $[NTf_2]^-$ anion in the PIL–IL membranes leads to higher CO_2 and H_2 solubilities compared to those of the membranes comprising the $[C(CN)_3]^-$ anion. As mentioned before, this behavior masks the higher H_2 diffusivities of composites with cyano-functionalized anion, somehow explaining the low influence of H_2 diffusivity on H_2 permeability results.

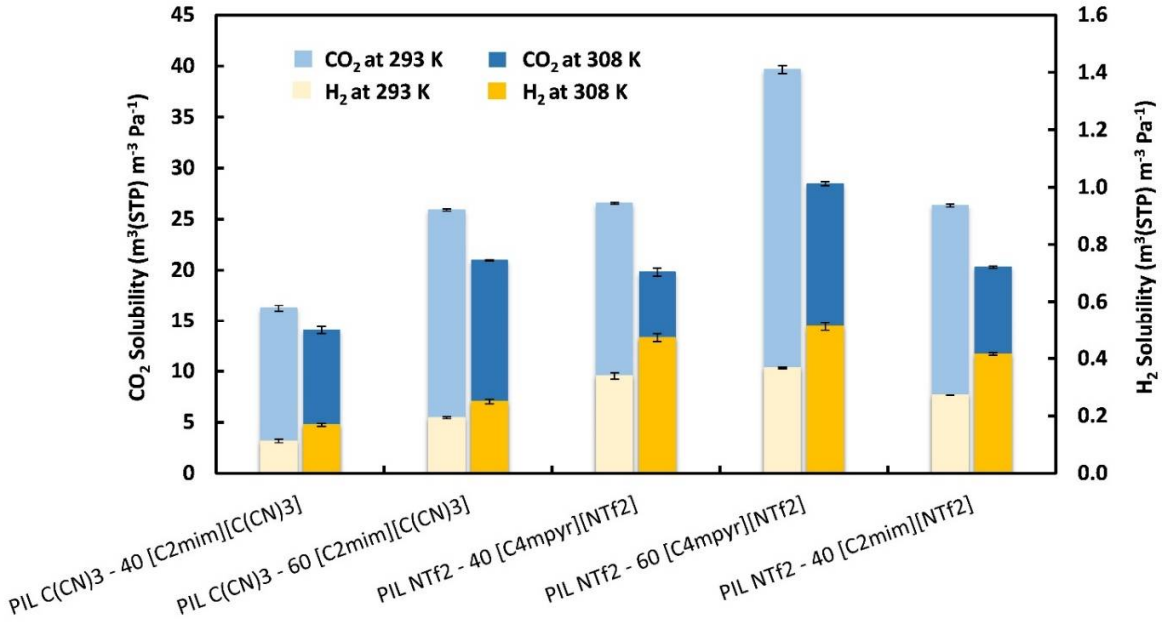

Figure 3 Gas solubilities (*S*) for the studied PIL–IL membranes at 293 K and 308 K.

Preprints (www.preprints.org) | NOT PEER-REVIEWED | Posted: 22 October 2018 doi:10.20944/preprints201810.0467.v1

Peer-reviewed version available at Membranes 2018, 8, 124; doi:10.3390/membranes8040124

3.2. CO_2/H_2 Separation Performance

The CO_2 and H_2 permeabilities and the ideal CO_2/H_2 permselectivities, determined at 293 K and 308 K, are summarized in Table 3. Amongst the studied PIL−IL membranes, those bearing the $[C(CN)_3]^-$ anion reveal slightly higher CO_2/H_2 permselectivities compared to those containing the $[NTf_2]^-$ anion. Actually, this behavior has also been observed in our previous works concerning the use of PIL–IL membranes for CO_2/N_2 and CO_2/CH_4 separation.[39,40,42] Moreover, from Table 3, it can be seen that CO_2/H_2 permselectivities decrease with increasing temperature. This result can be explained by the variations in CO_2/H_2 solubility selectivity with temperature, which leads to a decrease of CO_2/H_2 permselectivities as temperature increases [55]. In fact, CO_2/H_2 solubility selectivity through the studied composite membranes decreases from 78 – 145 at 293 K to 42 – 84 at 308 K. It can also be emphasized that CO_2/H_2 permselectivity seems to be controlled by a solubility mechanism, since CO_2/H_2 diffusivity selectivity (D CO_2/H_2) values are approximately equal to 0.1 at both temperatures while solubility selectivity (S CO_2/H_2) values range from 78 – 145 at 293 K and 42 – 84 at 308 K.

Table 3 Single gas permeabilities (P)[a] and ideal permselectivities (α) of the studied PIL–IL membranes.[b]

PIL-IL membrane	Gas Permeability (Barrer) (T = 293 K)			Gas Permeability (Barrer) (T = 308 K)		
	P CO_2 ± σ	P H_2 ± σ	α CO_2/H_2	P CO_2 ± σ	P H_2 ± σ	α CO_2/H_2
PIL $C(CN)_3$ – 40 $[C_2mim][C(CN)_3]$	139 ± 0.5	14.5 ± 0.2	9.6 ± 0.2	209 ± 0.9	25.7 ± 0.1	8.1 ± 0.1
PIL $C(CN)_3$ – 60 $[C_2mim][C(CN)_3]$	438 ± 2.1	29.1 ± 0.4	15.1 ± 0.3	505 ± 0.3	40.3 ± 1.1	12.5 ± 0.3
PIL NTf_2 – 40 $[C_4mpyr][NTf_2]$	119 ± 0.2	21.9 ± 0.1	5.4 ± 0.1	164 ± 1.6	34.4 ± 0.3	4.8 ± 0.1
PIL NTf_2 – 60 $[C_4mpyr][NTf_2]$	232 ± 2.2	29.8 ± 0.1	7.8 ± 0.1	288 ± 1.6	46.0 ± 0.1	6.3 ± 0.1
PIL NTf_2 – 40 $[C_2mim][NTf_2]$	214 ± 0.6	26.2 ± 0.1	8.2 ± 0.1	287 ± 2.4	43.8 ± 0.2	6.5 ± 0.1

[a] Barrer (1 Barrer = 10^{-10} $cm_{(STP)}^3$ cm cm^{-2} s^{-1} $cmHg^{-1}$). [b] The listed uncertainties represent the standard deviations (σ), based on three experiments.

The gas separation performance of the studied PIL–IL membranes is shown in Figure 4, where the CO_2/H_2 permselectivity is plotted against the permeability of the more permeable gas specie (CO_2). This graph displays a tradeoff (black line) between gas permeability and selectivity. These upper bound limits for several gas pairs were first developed by Robeson [56], who correlated data obtained from measurements carried out with polymeric membranes at low temperatures (298 – 308 K). Later, Rowe et al. [55] studied the influence of temperature on the tradeoff between gas permeability and permselectivity for different gas pairs. Thus, the upper bound at 300 K developed by Rowe et al. [55] for the CO_2/H_2 gas pair is represented in Figure 4 and was used to evaluate the performance of the studied PIL–IL membranes for biohydrogen purification (T = 308 K and 100 kPa).

Figure 4 clearly shows that all the studied PIL–IL membranes display CO_2/H_2 separation performances above the upper bound. The best CO_2/H_2 separation performance was obtained for the PIL–IL membrane composed of poly([Pyr_{11}][$C(CN)_3$]) and 60 wt% of [C_2mim][$C(CN)_3$] IL, which is in agreement to what has been observed in our recent works regarding the use of PIL-IL composites for CO_2/N_2 separation [40]. Literature data points for other reported PIL–IL membranes are also plotted in Figure 4 for comparison. The gas permeation measurements reported by Carlisle et al. [34] were performed at room temperature with a transmembrane pressure differential of 200 kPa. Also, their PIL–IL membranes were not prepared by solvent casting method but through UV polymerization by mixing different percentages of imidazolium-based IL monomers, cross-linking monomer and free IL [34]. From Figure 4, it can be seen that the PIL–IL membranes reported in the literature also present CO_2/H_2 separation performances above the upper bound for CO_2/H_2 gas pair at 300 K, but the PIL $C(CN)_3$ - 60 [C_2mim][$C(CN)_3$] membrane studied in this work still reveal superior CO_2/H_2 separation performance.

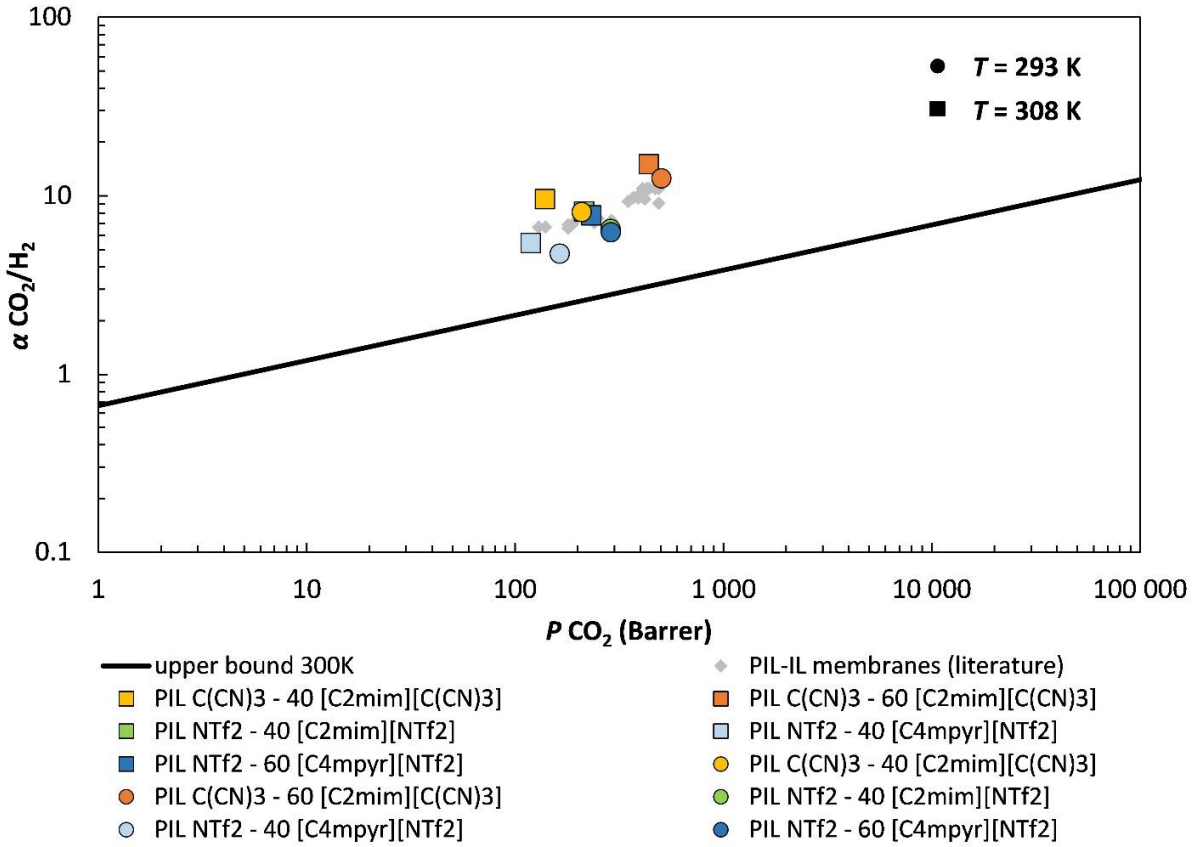

Figure 4 CO_2/H_2 separation performance of the studied PIL–IL membranes. The experimental error is within the data points. Data are plotted on a log–log scale and the upper bound at 300 K. is adapted from Rowe et al. [55]. Literature data points (◆) from other reported PIL–IL membranes are also displayed for comparison [34].

Peer-reviewed version available at Membranes 2018, 8, 124; doi:10.3390/membranes8040124

4. CONCLUSIONS

In this work, dense membranes containing a pyrrolidinium-based PIL combined with $[C(CN)_3]^-$ or $[NTf_2]^-$ anions and different quantities of free IL ($[C_2mim][C(CN)_3]$, $[C_4mpyr][NTf_2]$ or $[C_2mim][NTf_2]$) incorporated were prepared by solvent casting method and their CO_2 and H_2 permeation properties (permeability, diffusivity and solubility) measured and discussed at biohydrogen purification conditions ($\underline{T}$ = 308 K and 100 kPa of feed pressure). The CO_2 and H_2 permeation properties were also measured at $\underline{T}$ = 293 K and the effect of temperature on gas separation performance evaluated.

The PIL-IL membranes containing the $[NTf_2]^-$ anion presented the highest H_2 permeability and solubility values, while PIL-IL composites including the $[C(CN)_3]^-$ anion showed the highest H_2 diffusivities and CO_2/H_2 permselectivities. As previously reported, an increase in gas permeabilities, diffusivities and solubilities was observed with increasing temperature and the amount of IL, with exception of H_2 solubility, that showed the opposite behavior with temperature compared to what occurs in CO_2 solubility. Overall, all the studied PIL–IL membranes revealed similar or superior CO_2/H_2 separation performances compared to the few PIL-IL composites reported so far in literature. Particularly, at 308 K, the best result was obtained through the PIL $C(CN)_3$ – 60 IL $C(CN)_3$ composite membrane (CO_2 permeability of 505 Barrer and CO_2/H_2 selectivity of 12.5), that, as shown in our previous work, also presented remarkable results for CO_2/N_2 separation.

AUTHOR INFORMATION

***Corresponding Authors**

liliana.tome@itqb.unl.pt. Fax: +351 21 4411277. Tel: +351 21 4469714

isabel.marrucho@tecnico.ulisboa.pt. Fax: +351 21 8499242. Tel: +351 21 8413385

Notes

The authors declare no competing financial interest.

ACKNOWLEDGMENTS

Andreia S. L. Gouveia and Liliana C. Tomé are grateful to FCT (*Fundação para a Ciência e a Tecnologia*) for their Doctoral (SFRH/BD/116600/2016) and Post-doctoral (SFRH/BPD/101793/2014) research grants, respectively. This work was supported by FCT through the project PTDC/CTM-POL/2676/2014 and R&D units UID/QUI/00100/2013 (CQE) and UID/Multi/04551/2013 (GreenIT).

ABBREVIATIONS

Δp_d	Variation of downstream pressure
Δp_i	Pressure driving force
A	Effective membrane surface area
bioH_2	Biohydrogen
CO_2	Carbon Dioxide
D	Diffusivity
H_2	Hydrogen
H_2O	Water

Peer-reviewed version available at Membranes 2018, 8, 124; doi:10.3390/membranes8040124

H_2S	Hydrogen Sulfide
ILs	Ionic Liquids
J_i	Steady-state gas flux
ℓ	Membrane thickness
N_2	Nitrogen
O_2	Oxygen
P	Permeability
PILs	Poly(ionic liquid)s
R	Ideal Gas Law constant
S	Solubility
t	Time
T	Temperature
V^p	Permeate Volume
$\alpha_{i/j}$	Permselectivity
θ	Time-lag parameter

Cations

$[C_2mim]^+$	1-ethyl-3-methylimidazolium
$[C_4mpyr]^+$	1-butyl-3-methylpyrrolidinium

Anions

$[NTf_2]^-$	Bis(tri-fluoromethylsulfonyl)imide
$[C(CN)_3]^-$	Tricyanomethanide

REFERENCES

1. Mazloomi, K.; Gomes, C. Hydrogen as an energy carrier: Prospects and challenges. *Renewable and Sustainable Energy Reviews* **2012**, *16*, 3024-3033.
2. Das, D.; Veziroğlu, T.N. Hydrogen production by biological processes: a survey of literature. *International Journal of Hydrogen Energy* **2001**, *26*, 13-28.
3. Kalamaras, C.M.; Efstathiou, A.M. Hydrogen Production Technologies: Current State and Future Developments. *Conference Papers in Energy* **2013**, *2013*, 9.
4. Das, D.; Veziroglu, T.N. Advances in biological hydrogen production processes. *International Journal of Hydrogen Energy* **2008**, *33*, 6046-6057.
5. Manish, S.; Banerjee, R. Comparison of biohydrogen production processes. *International Journal of Hydrogen Energy* **2008**, *33*, 279-286.
6. Singh, L.; Wahid, Z.A. Methods for enhancing bio-hydrogen production from biological process: A review. *Journal of Industrial and Engineering Chemistry* **2015**, *21*, 70-80.
7. Alves, H.J.; Bley Junior, C.; Niklevicz, R.R.; Frigo, E.P.; Frigo, M.S.; Coimbra-Araújo, C.H. Overview of hydrogen production technologies from biogas and the applications in fuel cells. *International Journal of Hydrogen Energy* **2013**, *38*, 5215-5225.
8. Merkel, T.C.; Zhou, M.; Baker, R.W. Carbon dioxide capture with membranes at an IGCC power plant. *Journal of Membrane Science* **2012**, *389*, 441-450.
9. Dunikov, D.; Borzenko, V.; Blinov, D.; Kazakov, A.; Lin, C.Y.; Wu, S.Y.; Chu, C.Y. Biohydrogen purification using metal hydride technologies. *International Journal of Hydrogen Energy* **2016**, *41*, 21787-21794.
10. Sanders, D.F.; Smith, Z.P.; Guo, R.; Robeson, L.M.; McGrath, J.E.; Paul, D.R.; Freeman, B.D. Energy-efficient polymeric gas separation membranes for a sustainable future: A review. *Polymer* **2013**, *54*, 4729-4761.
11. Bakonyi, P.; Nemestóthy, N.; Ramirez, J.; Ruiz-Filippi, G.; Bélafi-Bakó, K. Escherichia coli (XL1-BLUE) for continuous fermentation of bioH2 and its separation by polyimide membrane. *International Journal of Hydrogen Energy* **2012**, *37*, 5623-5630.
12. Bakonyi, P.; Kumar, G.; Nemestóthy, N.; Lin, C.Y.; Bélafi-Bakó, K. Biohydrogen purification using a commercial polyimide membrane module: Studying the effects of some process variables. *International Journal of Hydrogen Energy* **2013**, *38*, 15092-15099.

13. Bakonyi, P.; Nemestóthy, N.; Bélafi-Bakó, K. Biohydrogen purification by membranes: An overview on the operational conditions affecting the performance of non-porous, polymeric and ionic liquid based gas separation membranes. *International Journal of Hydrogen Energy* **2013**, *38*, 9673-9687.
14. Basu, S.; Khan, A.L.; Cano-Odena, A.; Liu, C.; Vankelecom, I.F.J. Membrane-based technologies for biogas separations. *Chemical Society Reviews* **2010**, *39*, 750-768.
15. Mohamad, I.N.; Rohani, R.; Mastar@Masdar, M.S.; Mohd Nor, M.T.; Md. Jahim, J. Permeation properties of polymeric membranes for biohydrogen purification. *International Journal of Hydrogen Energy* **2016**, *41*, 4474-4488.
16. Pientka, Z.; Peter, J.; Zitka, J.; Bakonyi, P. Application of Polymeric Membranes in Biohydrogen Purification and Storage. *Current Biochemical Engineering* **2014**, *1*, 99-105.
17. Pientka, Z.; Peter, J.; Zitka, J.; Bakonyi, P. *Application of Polymeric Membranes in Biohydrogen Purification and Storage*; 2014; Vol. 1, pp. 99-105.
18. Kanehashi, S.; Kishida, M.; Kidesaki, T.; Shindo, R.; Sato, S.; Miyakoshi, T.; Nagai, K. CO2 separation properties of a glassy aromatic polyimide composite membranes containing high-content 1-butyl-3-methylimidazolium bis(trifluoromethylsulfonyl)imide ionic liquid. *Journal of Membrane Science* **2013**, *430*, 211-222.
19. Friess, K.; Jansen, J.C.; Bazzarelli, F.; Izák, P.; Jarmarová, V.; Kačírková, M.; Schauer, J.; Clarizia, G.; Bernardo, P. High ionic liquid content polymeric gel membranes: Correlation of membrane structure with gas and vapour transport properties. *Journal of Membrane Science* **2012**, *415-416*, 801-809.
20. Yuan, J.; Mecerreyes, D.; Antonietti, M. Poly(ionic liquid)s: An update. *Progress in Polymer Science* **2013**, *38*, 1009-1036.
21. Jeffrey Horne, W.; Andrews, M.A.; Shannon, M.S.; Terrill, K.L.; Moon, J.D.; Hayward, S.S.; Bara, J.E. Effect of branched and cycloalkyl functionalities on CO2 separation performance of poly(IL) membranes. *Separation and Purification Technology* **2015**, *155*, 89-95.
22. Bara, J.E.; Gabriel, C.J.; Hatakeyama, E.S.; Carlisle, T.K.; Lessmann, S.; Noble, R.D.; Gin, D.L. Improving CO2 selectivity in polymerized room-temperature ionic liquid gas

separation membranes through incorporation of polar substituents. *Journal of Membrane Science* **2008**, *321*, 3-7.

23. Bara, J.; Hatakeyama, E.; L. Gin, D.; D. Noble, R. Improving CO2 permeability in polymerized room ‐ temperature ionic liquid gas separation membranes through the formation of a solid composite with a room ‐ temperature ionic liquid. *Polym Advan Technol* **2008**, *19*, 1415-1420.
24. Bara, J.E.; Lessmann, S.; Gabriel, C.J.; Hatakeyama, E.S.; Noble, R.D.; Gin, D.L. Synthesis and Performance of Polymerizable Room-Temperature Ionic Liquids as Gas Separation Membranes. *Industrial & Engineering Chemistry Research* **2007**, *46*, 5397-5404.
25. Hu, X.; Tang, J.; Blasig, A.; Shen, Y.; Radosz, M. CO2 permeability, diffusivity and solubility in polyethylene glycol-grafted polyionic membranes and their CO2 selectivity relative to methane and nitrogen. *Journal of Membrane Science* **2006**, *281*, 130-138.
26. Hao, L.; Li, P.; Yang, T.; Chung, T.-S. Room temperature ionic liquid/ZIF-8 mixed-matrix membranes for natural gas sweetening and post-combustion CO2 capture. *Journal of Membrane Science* **2013**, *436*, 221-231.
27. Hudiono, Y.C.; Carlisle, T.K.; LaFrate, A.L.; Gin, D.L.; Noble, R.D. Novel mixed matrix membranes based on polymerizable room-temperature ionic liquids and SAPO-34 particles to improve CO2 separation. *Journal of Membrane Science* **2011**, *370*, 141-148.
28. Hudiono, Y.C.; Carlisle, T.K.; Bara, J.E.; Zhang, Y.; Gin, D.L.; Noble, R.D. A three-component mixed-matrix membrane with enhanced CO2 separation properties based on zeolites and ionic liquid materials. *Journal of Membrane Science* **2010**, *350*, 117-123.
29. Tomé, L.C.; Marrucho, I.M. Ionic liquid-based materials: a platform to design engineered CO2 separation membranes. *Chemical Society Reviews* **2016**, *45*, 2785-2824.
30. Sadeghpour, M.; Yusoff, R.; Aroua Mohamed, K. Polymeric ionic liquids (PILs) for CO2 capture. In *Reviews in Chemical Engineering*, 2017; Vol. 33, p 183.
31. Qian, W.; Texter, J.; Yan, F. Frontiers in poly(ionic liquid)s: syntheses and applications. *Chemical Society Reviews* **2017**, *46*, 1124-1159.
32. Ajjan, F.N.; Ambrogi, M.; Tiruye, G.A.; Cordella, D.; Fernandes, A.M.; Grygiel, K.; Isik, M.; Patil, N.; Porcarelli, L.; Rocasalbas, G., et al. Innovative polyelectrolytes/poly(ionic liquid)s for energy and the environment. *Polymer International* **2017**, *66*, 1119-1128.

33. Zulfiqar, S.; Sarwar, M.I.; Mecerreyes, D. Polymeric ionic liquids for CO2 capture and separation: potential, progress and challenges. *Polymer Chemistry* **2015**, *6*, 6435-6451.
34. Carlisle, T.K.; Nicodemus, G.D.; Gin, D.L.; Noble, R.D. CO2/light gas separation performance of cross-linked poly(vinylimidazolium) gel membranes as a function of ionic liquid loading and cross-linker content. *Journal of Membrane Science* **2012**, *397–398*, 24-37.
35. Shaligram, S.V.; Wadgaonkar, P.P.; Kharul, U.K. Polybenzimidazole-based polymeric ionic liquids (PILs): Effects of 'substitution asymmetry' on CO2 permeation properties. *Journal of Membrane Science* **2015**, *493*, 403-413.
36. K. Carlisle, T.; F. Wiesenauer, E.; D. Nicodemus, G.; L. Gin, D.; D. Noble, R. Ideal CO2/Light Gas Separation Performance of Poly(vinylimidazolium) Membranes and Poly(vinylimidazolium)-Ionic Liquid Composite Films. *Industrial & Engineering Chemistry Research* **2012**, *52*, 1023–1032.
37. Li, P.; Paul, D.R.; Chung, T.-S. High performance membranes based on ionic liquid polymers for CO2 separation from the flue gas. *Green Chemistry* **2012**, *14*, 1052-1063.
38. Li, P.; Pramoda, K.P.; Chung, T.-S. CO2 Separation from Flue Gas Using Polyvinyl-(Room Temperature Ionic Liquid)–Room Temperature Ionic Liquid Composite Membranes. *Industrial & Engineering Chemistry Research* **2011**, *50*, 9344-9353.
39. Tomé, L.C.; Mecerreyes, D.; Freire, C.S.R.; Rebelo, L.P.N.; Marrucho, I.M. Pyrrolidinium-based polymeric ionic liquid materials: New perspectives for CO2 separation membranes. *Journal of Membrane Science* **2013**, *428*, 260-266.
40. Tomé, L.C.; Isik, M.; Freire, C.S.R.; Mecerreyes, D.; Marrucho, I.M. Novel pyrrolidinium-based polymeric ionic liquids with cyano counter-anions: High performance membrane materials for post-combustion CO2 separation. *Journal of Membrane Science* **2015**, *483*, 155-165.
41. Tomé, L.C.; Gouveia, A.S.L.; Freire, C.S.R.; Mecerreyes, D.; Marrucho, I.M. Polymeric ionic liquid-based membranes: Influence of polycation variation on gas transport and CO2 selectivity properties. *Journal of Membrane Science* **2015**, *486*, 40-48.
42. Teodoro, R.M.; Tomé, L.C.; Mantione, D.; Mecerreyes, D.; Marrucho, I.M. Mixing poly(ionic liquid)s and ionic liquids with different cyano anions: Membrane forming

ability and CO2/N2 separation properties. *Journal of Membrane Science* **2018**, *552*, 341-348.

43. Tomé, L.C.; Florindo, C.; Freire, C.S.; Rebelo, L.P.; Marrucho, I.M. Playing with ionic liquid mixtures to design engineered CO2 separation membranes. *Physical Chemistry Chemical Physics* **2014**, *16*, 17172-17182.
44. Pont, A.-L.; Marcilla, R.; De Meatza, I.; Grande, H.; Mecerreyes, D. Pyrrolidinium-based polymeric ionic liquids as mechanically and electrochemically stable polymer electrolytes. *Journal of Power Sources* **2009**, *188*, 558-563.
45. Wijmans, J.G.; Baker, R.W. The solution-diffusion model: a review. *Journal of Membrane Science* **1995**, *107*, 1-21.
46. Matteucci, S.; Yampolskii, Y.; Freeman, B.D.; Pinnau, I. Transport of Gases and Vapors in Glassy and Rubbery Polymers. In *Materials Science of Membranes for Gas and Vapor Separation*, John Wiley & Sons, Ltd: 2006; pp. 1-47.
47. Rutherford, S.W.; Do, D.D. Review of time lag permeation technique as a method for characterisation of porous media and membranes. *Adsorption-Journal of the International Adsorption Society* **1997**, *3*, 283-312.
48. Wang, S.; Li, X.; Wu, H.; Tian, Z.; Xin, Q.; He, G.; Peng, D.; Chen, S.; Yin, Y.; Jiang, Z., et al. Advances in high permeability polymer-based membrane materials for CO2 separations. *Energy & Environmental Science* **2016**, *9*, 1863-1890.
49. Raeissi, S.; Peters, C.J. Understanding temperature dependency of hydrogen solubility in ionic liquids, including experimental data in [bmim][Tf2N]. *AIChE Journal* **2012**, *58*, 3553-3559.
50. Kumełan, J.; Pérez-Salado Kamps, Á.; Tuma, D.; Maurer, G. Solubility of H2 in the Ionic Liquid [bmim][PF6]. *Journal of Chemical & Engineering Data* **2006**, *51*, 11-14.
51. Finotello, A.; Bara, J.E.; Camper, D.; Noble, R.D. Room-Temperature Ionic Liquids: Temperature Dependence of Gas Solubility Selectivity. *Industrial & Engineering Chemistry Research* **2008**, *47*, 3453-3459.
52. Kumełan, J.; Tuma, D.; Pérez-Salado Kamps, Á.; Maurer, G. Solubility of the Single Gases Carbon Dioxide and Hydrogen in the Ionic Liquid [bmpy][Tf2N]. *Journal of Chemical & Engineering Data* **2010**, *55*, 165-172.

53. Raeissi, S.; Florusse, L.J.; Peters, C.J. Hydrogen Solubilities in the IUPAC Ionic Liquid 1-Hexyl-3-methylimidazolium Bis(Trifluoromethylsulfonyl)Imide. *Journal of Chemical & Engineering Data* **2011**, *56*, 1105-1107.

54. Robeson, L.M.; Smith, Z.P.; Freeman, B.D.; Paul, D.R. Contributions of diffusion and solubility selectivity to the upper bound analysis for glassy gas separation membranes. *Journal of Membrane Science* **2014**, *453*, 71-83.

55. Rowe, B.W.; Robeson, L.M.; Freeman, B.D.; Paul, D.R. Influence of temperature on the upper bound: Theoretical considerations and comparison with experimental results. *Journal of Membrane Science* **2010**, *360*, 58-69.

56. Robeson, L.M. The upper bound revisited. *Journal of Membrane Science* **2008**, *320*, 390-400.

Preprints (www.preprints.org) | NOT PEER-REVIEWED | Posted: 22 October 2018 doi:10.20944/preprints201810.0467.v1

Peer-reviewed version available at Membranes 2018, 8, 124; doi:10.3390/membranes8040124

Table of Contents

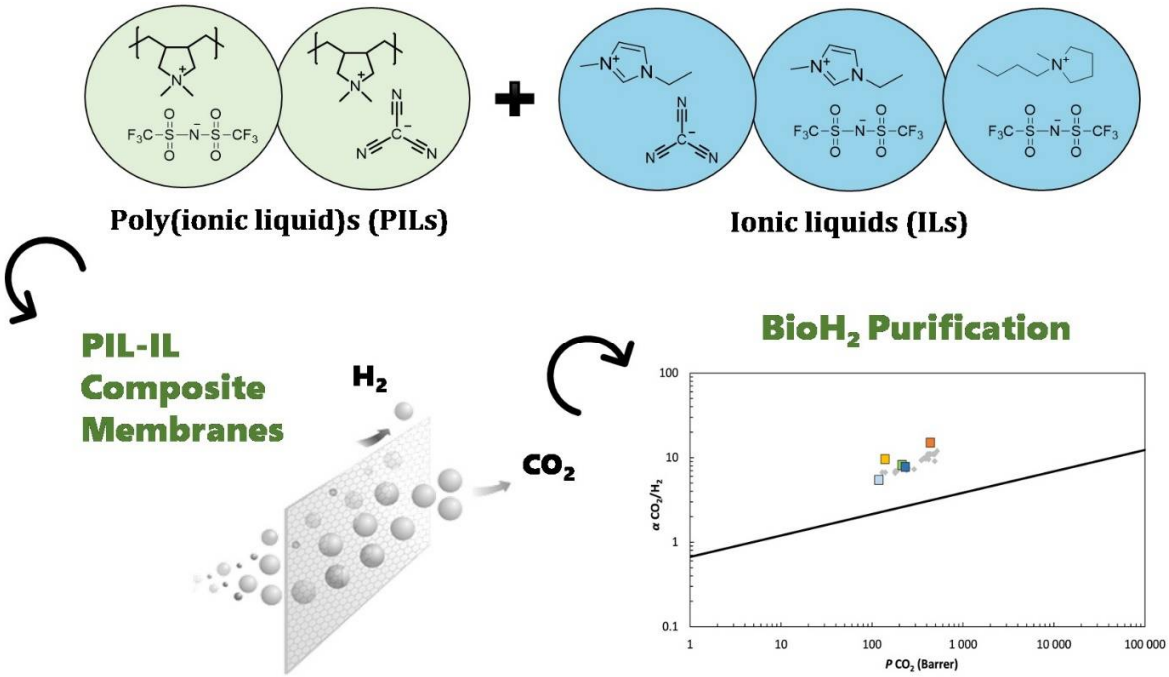

"Towards biohydrogen separation using poly(ionic liquid)/ionic liquid composite membranes"

Andreia S.L. Gouveia,[a,b] Lucas Ventaja,[a] Liliana C. Tomé,[a,b] and Isabel M. Marrucho[a,b*]*